CHEMISTRY
A EUROPEAN JOURNAL

DOI: 10.1002/chem.201003550

VIP

Rates of Water Exchange for Two Cobalt(II) Heteropolyoxotungstate Compounds in Aqueous Solution

C. André Ohlin,[a, b] Stephen J. Harley,[a, b] J. Gregory McAlpin,[a, b] Rosalie K. Hocking,*[c] Brandon Q. Mercado,[a] Rene L. Johnson,[a, b] Eric M. Villa,[a, d] Mary Kate Fidler,[d] Marilyn M. Olmstead,[a] Leone Spiccia,*[c] R. David Britt,*[a] and William H. Casey*[a, b]

Abstract: Polyoxometalate ions are used as ligands in water-oxidation processes related to solar energy production. An important step in these reactions is the association and dissociation of water from the catalytic sites, the rates of which are unknown. Here we report the exchange rates of water ligated to Co^{II} atoms in two polyoxotungstate sandwich molecules using the ^{17}O-NMR-based Swift–Connick method. The compounds were the $[Co_4(H_2O)_2(B\text{-}\alpha\text{-}PW_9O_{34})_2]^{10-}$ and the larger $\alpha\beta\beta\alpha\text{-}[Co_4(H_2O)_2(P_2W_{15}O_{56})_2]^{16-}$ ions, each with two water molecules bound *trans* to one another in a Co^{II} sandwich between the tungstate ligands. The clusters, in both solid and solution state, were characterized by a range of methods, including NMR, EPR, FT-IR, UV-Vis, and EXAFS spectroscopy, ESI-MS, single-crystal X-ray crystallography, and potentiometry. For $[Co_4(H_2O)_2(B\text{-}\alpha\text{-}PW_9O_{34})_2]^{10-}$ at pH 5.4, we estimate: $k^{298}=1.5(5)\pm0.3\times10^6\,s^{-1}$, $\Delta H^{\neq}=39.8\pm0.4\,kJ\,mol^{-1}$, $\Delta S^{\neq}=+7.1\pm1.2\,J\,mol^{-1}\,K^{-1}$ and $\Delta V^{\neq}=5.6\pm1.6\,cm^3\,mol^{-1}$. For the Wells–Dawson sandwich cluster ($\alpha\beta\beta\alpha\text{-}[Co_4(H_2O)_2(P_2W_{15}O_{56})_2]^{16-}$) at pH 5.54, we find: $k^{298}=1.6(2)\pm0.3\times10^6\,s^{-1}$, $\Delta H^{\neq}=27.6\pm0.4\,kJ\,mol^{-1}$ $\Delta S^{\neq}=-33\pm1.3\,J\,mol^{-1}\,K^{-1}$ and $\Delta V^{\neq}=2.2\pm1.4\,cm^3mol^{-1}$ at pH 5.2. The molecules are clearly stable and monospecific in slightly acidic solutions, but dissociate in strongly acidic solutions. This dissociation is detectable by EPR spectroscopy as $S=3/2$ Co^{II} species (such as the $[Co(H_2O)_6]^{2+}$ monomer ion) and by the significant reduction of the Co–Co vector in the XAS spectra.

Keywords: cobalt · oxidation · polyoxometalates · tungsten · water

Introduction

Polyoxometalate ions have an enormous range of uses (see Hill[1] for a review) from oxidation catalysts[2–4] to antiprion[5] and anti-viral drugs[6] to photocatalysts.[7] Particularly interesting are polyoxometalate molecules with transition-metal oxides sandwiched as a layer between tungstate lig-

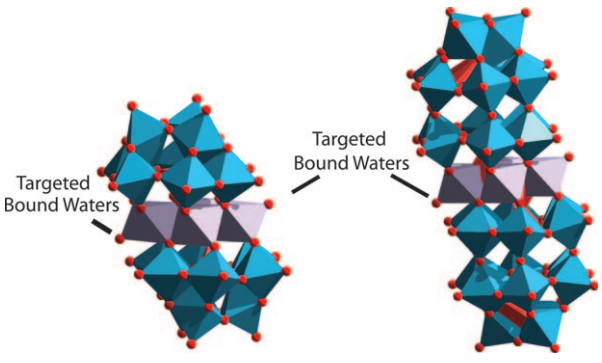

Figure 1. The polyoxometalate ions used in this study. The Co^{II} octahedra are shown as violet, the tungstate ligands as blue and oxygen atoms are identified as red spheres. For the two sandwich compounds (left = $[Co_4(H_2O)_2(B\text{-}\alpha\text{-}PW_9O_{34})_2]^{10-}$; right = $\alpha\beta\beta\alpha\text{-}Co_4(H_2O)_2(PW_{15}O_{56})_2]^{16-}$) the central Co^{II} is organized in a brucite-like layer of edge-shared $Co(O)_6$ octahedra. Bound water sites are indicated.

[a] Dr. C. A. Ohlin, Dr. S. J. Harley, J. G. McAlpin, B. Q. Mercado, R. L. Johnson, Dr. E. M. Villa, Prof. M. M. Olmstead, Prof. R. D. Britt, Prof. W. H. Casey
Department of Chemistry, University of California
Davis, California 95616 (USA)
Fax: (+1) 530-752-8995
E-mail: rdbritt@ucdavis.edu
whcasey@ucdavis.edu

[b] Dr. C. A. Ohlin, Dr. S. J. Harley, J. G. McAlpin, R. L. Johnson, Prof. W. H. Casey
Department of Geology, University of California
Davis, California 95616 (USA)

[c] Dr. R. K. Hocking, Prof. L. Spiccia
School of Chemistry
Australian Centre of Excellence for Electromaterials Science
and Monash Centre for Synchrotron Science
Monash University, Victoria, 3800 (Australia)
Fax: (+61) 3-9905-4597
E-mail: leone.spiccia@monash.edu
rosalie.hocking@monash.edu

[d] Dr. E. M. Villa, M. K. Fidler
Present address: Department of Civil Engineering and Geosciences
University of Notre Dame, Notre Dame (Indiana)

Supporting information for this article is available on the WWW under http://dx.doi.org/10.1002/chem.201003550. It contains a range of spectroscopic data and X-ray crystallographic files.

ands (Figure 1), as the great diversity of available polyoxometalate structures and electronic motifs can allow for fine tuning of the catalytic activity. These compounds have already been shown to be effective oxidation catalysts, can activate molecular oxygen,[2,3] and recently generated great excitement as potential catalysts for chemically driven water oxidation.[8,9] The structural similarity of these sandwich compounds to some minerals also makes them a particularly appealing topic of investigation. For example, the central tetracobalt moiety in the water-oxidation catalyst reported by Yin et al.[8] strongly resembles a brucite-like motif, such as one might find in a clay or mica. Not surprisingly, some of these layered cobalt structures themselves have been shown to be efficient water-oxidation catalysts.[10,11]

Our goal is to better understand how these motifs react in water and by focusing on the rates of ligand substitution. In this sense we are responding to the call by Hill[7] for better physicochemical characterization of polyoxometalate ions in solution, including their reaction dynamics. Interestingly, Yin et al. did not observe water-oxidation catalysis when the larger Wells–Dawson derivative $[Co_4(H_2O)_2(\alpha,\alpha\text{-}P_2W_{15}O_{56})_2]^{16-}$ was employed,[8] in spite of having a cobalt tetramer core identical to that in $[Co_4(H_2O)_2(B\text{-}\alpha\text{-}PW_9O_{34})_2]^{10-}$; this result suggests that details of the ligand could play a crucial role in tuning the catalytic efficiency and/or stability of the complex. The water-oxidation site is likely to be situated on the two terminal cobalt atoms, which each have an aqua ligand coordinated. Herein, we determine the rates of water exchange at the Co^{II} sites in a series of similar polyoxometalates in an effort to advance an understanding of this important chemistry.

Experimental Section

Synthesis: The smaller molecule was synthesized as $K_{10}[Co_4(H_2O)_2(\alpha\text{-}PW_9O_{34})_2]\cdot 26H_2O$ (**1**) (Figure 1) according to the method suggested by Weakley et al.[12] and modified by Finke et al.[13] The larger molecule was the Wells–Dawson sandwich, $Na_{16}[Co_4(H_2O)_2(\alpha\text{-}P_2W_{15}O_{56})_2]\cdot 52\ H_2O$ (**2**), and was prepared by complexation of cobalt(II) with $Na_{12}[\alpha\text{-}PW_{15}O_{56}]$,[13] itself synthesized according to Contant.[14] Crystals were washed repeat-

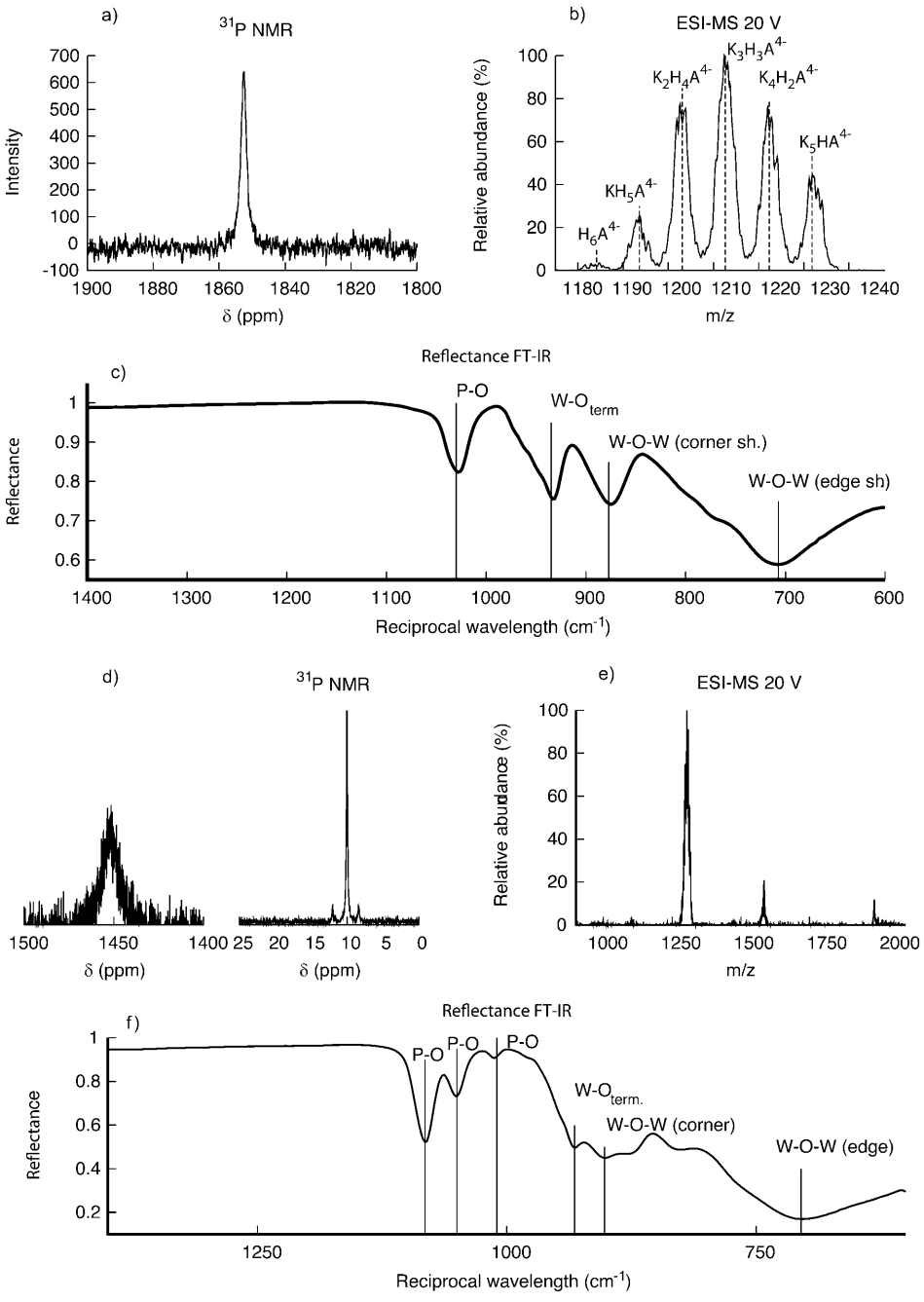

Figure 2. a) ^{31}P NMR spectrum of $[Co_4(H_2O)_2(B\text{-}\alpha\text{-}PW_9O_{34})_2]^{10-}$ at pH 7.2 b) Mass spectrum (ESI-MS) of the compound at the same pH showing the $z=4^-$ signals ($A=[Co_4(H_2O)_2(B\text{-}\alpha\text{-}PW_9O_{34})_2]^{10-}$); c) reflectance-mode FTIR spectrum of $K_{10}[Co_4(H_2O)_2(\alpha\text{-}PW_9O_{34})_2]\cdot n\,H_2O$. d) ^{31}P NMR spectrum of $Co_4(H_2O)_2(\alpha\text{-}P_2W_{15}O56)_2^{16-}$ (aq) at pH 4.9. Two peaks are identified corresponding to ^{31}P atoms proximal and distal to the Co^{II} sandwich. e) Mass spectrum (ESI-MS) of the compound showing the entire spectrum at near-neutral pH. f) Reflectance-mode FTIR spectrum of $Na_{16}[Co_4(H_2O)_2(\alpha\text{-}P_2W_{15}O_{56})_2]\cdot n\,H_2O$.

edly with cold, concentrated, aqueous sodium chloride solutions until the filtrate was colorless, ground to a powder, followed by repeated washing and drying.

FT-IR and ^{31}P NMR characterization: The reflectance FT-IR spectra of **1** and **2** (Figure 2) were obtained on a Bruker Tensor 27 spectrometer. The spectrum of **1** is identical to that reported by Finke et al.,[13] with a single P–O band, in addition to bands attributed to W=O (terminal), W-O-W (corner-sharing octahedra), and W-O-W (edge-sharing octahedra) groups. The ^{31}P NMR spectrum of **1** at different pH conditions showed a single broad signal between 1840 and 1900 ppm, depending on pH and temperature, consistent with the assignment as $[Co_4(H_2O)_2(B\text{-}\alpha\text{-}PW_9O_{34})_2]^{10-}$.

The reflectance FT-IR spectrum of **2** had an additional weak band that was attributable to P–O stretches at 1010 cm^{-1}. The absence of other unassigned bands, combined with other methods of analysis (below), also indicated that the product was pure. The weak P–O band is due to the presence of isomers, one of which is more abundant than the other. This conclusion is supported by ^{31}P NMR spectroscopy, which showed three signals in the 10–25 ppm region at neutral pH. Two of these, with relative areas of 1:1, can be assigned to the phosphorus atoms farthest removed from the cobalt tetramer in the $\alpha\beta\beta\beta$-$[Co_4(H_2O)_2(P_2W_{15}O_{56})_2]^{16-}$ species, while the main signal corresponds to the symmetrical $\alpha\beta\beta\alpha$-$[Co_4(H_2O)_2(P_2W_{15}O_{56})_2]^{16-}$ species.[15]

The changes in ^{31}P NMR spectra as a function of solution pH are consistent with the conclusions about isomerization of Ruhlmann et al.[15] In addition, ^{31}P NMR signals corresponding to the phosphorus atoms closer to the cobalt tetramer were only reliably observed in solutions with concentrations above 5 mM, owing to the significant broadening induced (600–1900 Hz) in these signals due to the proximity to the paramagnetic cobalt atoms. These signals were found in the 1190 to 1600 ppm region, again consistent with Ruhlmann et al.[15]

Chemical analyses: Elemental analyses were carried out by Galbraith Laboratories, Inc. (Knoxville, TN). Elemental analysis calcd (%) for $K_{10}[Co_4(H_2O)_2(PW_9O_{34})_2]$: Co 4.22, K 6.97, P 1.11, W 59.2; found: Co 4.60, K 7.38, P 0.82, W 58.8. Elemental analysis calcd (%) for $Na_{16}[Co_4(H_2O)_2(P_2W_{15}O_{56})_2]$: Co 2.62, Na 4.08, P 1.38, W 61.3; found: Co 2.65, Na 4.76, P 1.01, W 58.6. Thermal gravimetry showed 52 ± 0.5 moles of crystal water per mol of **2**.

Potentiometric titrations and UV/Vis characterization: These were carried out using standardized 0.112 M $HClO_4$ and 0.100 M NaOH solutions on a Metrohm 718 STAT Titrino auto-titrator. All sample solutions contained 0.10 M in $NaClO_4$ and were degassed with nitrogen prior to use. UV/Vis measurements were carried out on a Varian Cary 300 spectrophotometer. The amount of uncompensated charge resulting was calculated from Equation (1), which is a charge-balance equation that includes the analyzed concentrations of protons and hydroxide, and the known concentrations of counterions added in the titration (Figure 3).

$$Z = \frac{[H^+] + [Na^+] - [ClO_4^-] - [OH^-]}{[CoPOM_{Tot}]} \quad (1)$$

The counterion concentrations are all adjusted for dilution, but the Z values were relatively insensitive to values of activity coefficients. Inclusion of reasonable activity coefficients ($\gamma_{OH^-,Na^+,ClO_4^-} = 0.8$–$0.76$; $\gamma_{H^+} = 0.76$–0.73) for $I = 0.1$ M indicates less than 10% difference in the absolute values of Z and no difference in the amounts of hysteresis. (Note that the polyoxometalate concentrations were left out of the ionic-strength calculation because of their large size and anomalously high charge, which of course must be squared in calculation of ionic strength and activity coefficients.) The Z data were interpretable to indicate pK_a values by fitting to a two-site protonation equilibria.

Electrospray-ionization mass spectrometry (ESI-MS): Spectra were acquired in negative mode on an HP Agilent MSD G1956b single-quadrupole electrospray-ionization mass spectrometer (Figure 2b) equipped with a syringe pump for direct injection of solutions into the spray chamber at 40 μL min^{-1}. The cone voltage was varied from 0 to 300 V in 10 V steps at intervals of 1 min. For **1**, negative-mode electrospray-ionization mass spectrometry showed primarily a series of signals corresponding to $K_{(6-x)}H_x[Co_4(H_2O)_2(PW_9O_{34})_2]^{4-}$ ($1 \le x \le 6$) ions at low cone voltages

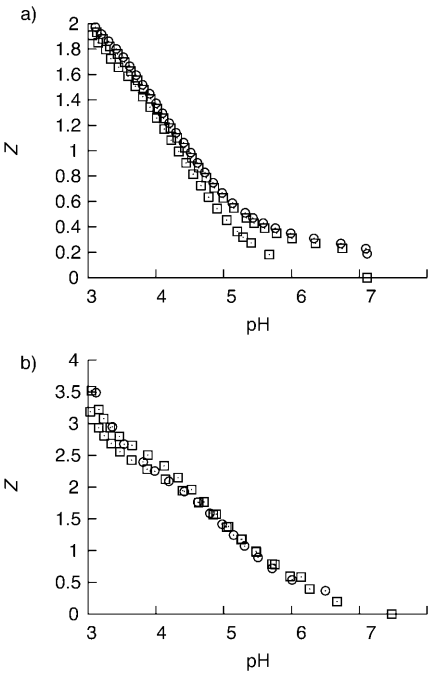

Figure 3. Potentiometric titration to measure the uncompensated charge (Z) in solutions of **1** (top) and **2** (bottom). The titration of **1** exhibited hysteresis, or was irreversible, at pH < 3 and pH > 7, while the titration of **2** was reversible over a much larger range of pH. Titration to lower pH values is shown as squares and back titration to higher pH in circles.

(<40 V) and collision-induced dissociation products, including $[KW_xO_{3x+1}]^-$ and $[PW_xO_{3x+3}]^-$, at higher cone voltages, establishing the identity and purity of **1** (see the Supporting Information).

NMR spectroscopy: Nuclear magnetic resonance solution measurements were carried out on a Bruker Avance DRX 500 MHz (11.75 T, ^{17}O 67.8 MHz; ^{31}P 202.4 MHz) spectrometer equipped with a 5 mm broadband probe. Temperature readings were obtained by a thermocouple reader connected to a dummy sample containing distilled water and a copper–constantan thermocouple. Spectra were acquired by averaging 512 scans with a pulse width of 10 μs, a recycle delay of 100 ms and a sweep width of 10 kHz with the carrier frequency set at 331 ppm. Samples were prepared in 0.1 M $NaClO_4$ and set to the desired pH by addition of 0.112 M $HClO_4$ in 0.10 M $NaClO_4$. An aliquot of the sample (0.6 mL) was transferred to a 5 mm NMR tube and 10 μL $H_2{}^{17}O$ (40%) added. In all cases, the standard solution was a 0.1 M $NaClO_4$ solution at pH 3.4, acidified to this pH with a small amount of $HClO_4$.

High-pressure NMR experiments were carried out on a wide-bore Bruker Avance (11.7 T) spectrometer that had a custom-built high-pressure probe with interchangeable ^{17}O NMR and ^{31}P probe heads. The probe pressure was generated with a high-pressure syringe pump by using a home-built valve system to maintain and regulate pressures throughout the experiment. *iso*-Hexane was used as the pressure conduit and pressures were continuously monitored and never allowed to fluctuate more than 0.5% during data acquisition. The temperature was kept constant by means of a circulating water bath and was monitored with a type-T thermocouple situated in the probe body near the probe head and at pressure. Thermal equilibrium was established after each pressure jump before data was acquired.

Rates were estimated via a Swift–Connick formalism.[16] Briefly, a two-site exchange mechanism in the dilute-solution limit allows for the peak widths to be interpreted by using a simplified form of the steady-state Bloch–McConnell equations [Eq. (2)].

$$\frac{1}{T_{2r}} = \frac{\pi}{P_m}(\Delta\nu_{obs} - \Delta\nu_{solvent}) = \frac{1}{\tau_m}\left(\frac{T_{2m}^{-2} + (T_{2m}\tau_m)^{-1} + \Delta\omega_m^2}{(T_{2m}^{-1}\tau_m^{-1})^2 + \Delta\omega_m^2}\right) \quad (2)$$

In Equation (2), T_{2r} is the reduced T_2, P_m is the mole fraction of bound water molecules divided by the mole fraction of solvent water. For example, this parameter, P_m, is the number of exchanging sites (e.g., six in $Co(H_2O)_6^{2+}$) multiplied by the concentration (e.g., 0.001 M) of the exchanging complex, divided by the molar concentration of water (55.56 M). τ_m is the exchange time, which relates directly to the rate coefficient, $\tau_m = 1/k_{ex}$. The $(\Delta\nu_{obs} - \Delta\nu_{solvent})$ term is the experimentally observed difference in peak width of the bulk-water signal with, and without, the paramagnetic complex present, and $\Delta\omega_m$ is the difference in resonance frequency of bulk solvent and solvent in the first coordination sphere of the polyoxometalate ion.

For paramagnetic Co^{II}, there is a temperature and pH region for which $T_{2m}^{-1} \gg \Delta\omega^2$, τ_m^{-1} in Equation (2) so that the equation may be rewritten as: $1/T_{2r} = 1/\tau_m$. We chose temperatures and pH conditions where this approximation is valid (Figure 4). Under these conditions the activation enthalpy ($\Delta H^{\neq}$) and entropy ($\Delta S^{\neq}$) for the exchange process could be extracted by plotting $\ln(1/T_{2r})$ versus $1/T$ (K) [Eq. (3)].

$$\frac{1}{T_{2r}} = \left(\frac{k_B T}{h}\right) e^{\left(\frac{\Delta S^{\neq}}{R} - \frac{\Delta H^{\neq}}{RT}\right)} \quad (3)$$

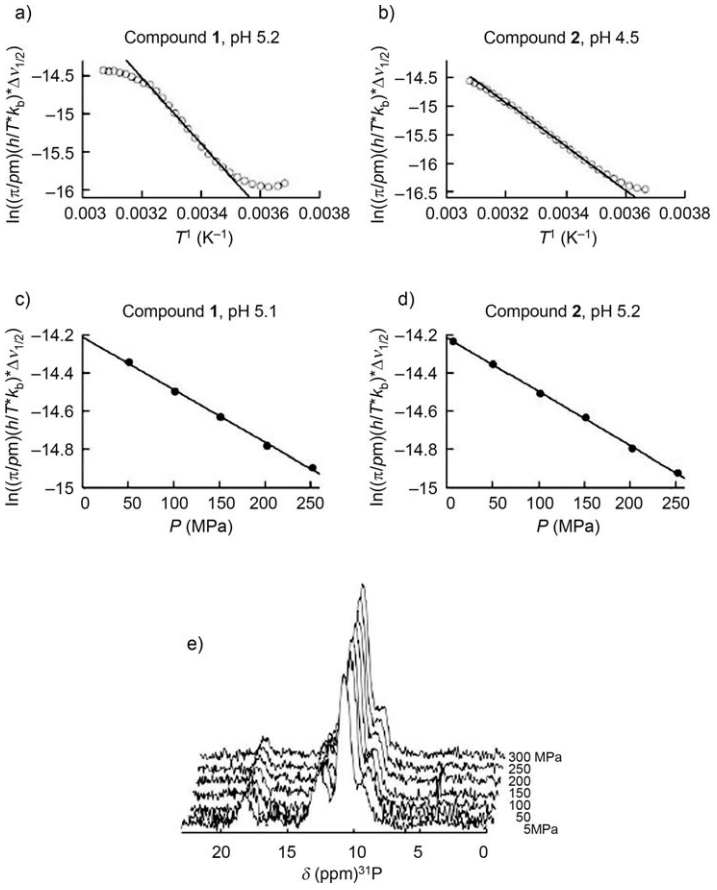

Figure 4. a), b) Line-width parameters derived for **1** and **2** from ^{17}O-NMR spectra as a function of temperature in the region of the Swift–Connick treatment at which line widths respond to rates of exchange of bound waters. c), d) Variation in rates for compounds **1** and **2** with pressure, at constant pH, used to determine an activation volume. e) High-pressure ^{31}P NMR data demonstrate that **2** is stable over the pressure range at this pH condition. The ^{31}P NMR peaks are assignable to the αββα and αβββ isomers of compound **2**.

The Swift–Connick equations, however, are nonlinear and, depending on the temperature, they include regions where the approximation that $T_{2m}^{-1} \gg \Delta\omega^2$, τ_m^{-1} in Equation (2) is no longer valid. At the higher pH region of this study (pH > 7.5), changes in line width at low temperature became insensitive to changes in temperature, precluding the determination of rates.

The dependence of T_{2r} and k_{ex} on pressure at a temperature where $T_{2m}^{-1} \gg \Delta\omega^2$, τ_m^{-1} in Equation (2) was also investigated by using a home-built high-pressure probe with interchangeable tuning circuits for either ^{17}O or ^{31}P. The functional dependence of exchange with pressure yields an activation volume [$\Delta V^{\neq}$: Eq. (4)][17–20]

$$\left(\frac{\partial \ln(k_{ex}(P))}{\partial p}\right)_T = -\frac{\Delta V^{\neq}}{RT} \quad (4)$$

Crystallographic data collection and refinement for (1) and (2): Crystals of $K_{10}[Co_4(H_2O)_2(\alpha\text{-}PW_9O_{34})_2]\cdot 26H_2O$ (**1**) were obtained by slow freezing of an aqueous solution in an EPR tube. A purple parallelepiped crystal of dimensions 0.04 mm × 0.06 mm × 0.06 mm was mounted in the 90(2) K cold stream provided by a Cryo Industries of America Cryocool-LN2 low-temperature apparatus on the goniometer head of a Bruker SMART ApexII DUO. Diffraction data were collected with use of $Mo_{K\alpha}$ radiation and corrected for absorption by a multiscan method using the program SADABS.[21] A total of 90333 data were collected, of which 11964 were unique [R(int) = 0.069]. The structure was solved by direct methods using SHELXS97 and refined by full-matrix least-squares on F^2 using SHELXL97[21] using 369 parameters. In the final cycles of refinement all oxygen atoms were kept isotropic. Hydrogen atoms were not located. There is disorder in one of the five K^+ ion sites. This was modeled with four positions: K5A/K5B/K5C/K5D with occupancies of 0.17/0.15/0.33/0.35, respectively. The compound should have 13 waters of hydration in the asymmetric unit. However, only 11.5 hydrate positions were reliably located. The top 50 difference map peaks are in the vicinity of tungsten atoms. The formula is reported below with the expected number of hydrogen and oxygen atoms. Crystal data were: $H_{56}Co_4K_{10}O_{96}P_2W_{18}$, M_w = 5590.41 amu, monoclinic, $P2_1/n$, a = 11.7808(5), b = 16.7304(7), c = 21.0609(9) Å, β = 100.290(2)°, V = 4084.3(3) Å^3, T = 90(2) K, Z = 2, ρ_{calcd} = 4.546, R_1 [$I > 2\sigma(I)$] = 0.0373, wR_2 (all data) = 0.1030, GOF (on F^2) = 1.049.

Crystals of $Na_{16}[Co_4(H_2O)_2(\alpha\text{-}P_2W_{15}O_{56})_2]\cdot 52H_2O$, (**2**) were obtained in the synthesis procedure during the cooling step (as for **1**, above). A colorless plate of dimensions 0.07 mm × 0.07 mm × 0.018 mm was mounted in the 100(2) K nitrogen coldstream provided by an Oxford Cryostream low-temperature apparatus on the goiniometer head of a Bruker D8 diffractometer equipped with an Apex II CCD detector on beamline 11.3.1 at the Advanced Light Source at Lawrence Berkeley Laboratory. Diffraction data were collected using synchrotron radiation monochromated with silicon(111) and a wavelength of 0.77490 Å. A total of 41963 data were collected, of which 16117 were unique [R(int) = 0.0705]. The data was corrected for absorption, and the structure solved and refined by the method given for **1**. Final refinement employed all data, 120 restraints, and 942 parameters. The structure contains disorder in the cap of three of the tungsten atoms, namely W1, W2, and W3. The disorder represents co-existence of two isomers. Consistent with the formalism of Anderson et al.[22] these are termed α,β,β,α and α,β,β,β, (the second and third 'β' refer to the Co^{II} sandwich, the first and last α or β refer to the cap; see Figure 2 in the paper by Anderson et al.[22]). To model the disorder, the cap and three of its O atoms were rotated by 60° and reinserted as a rigid group during refinement. The α–β cap arrangement refined to 15% occupancy and was subsequently fixed at this value. However, there are three oxygen positions not accounted for in the α–β form. These are at sites too close to other full-occupancy atoms.

All the atoms of the anion were assigned anisotropic thermal ellipsoids except for the disordered fragment. A similarity restraint was applied to the anisotropic thermal parameters. There are eight Na atoms in the model, of which 4.5 are ordered and at full occupancy (one of these resides on a center of inversion). The remainders were selected based on position and assigned partial occupancy values in accordance with rea-

sonable thermal ellipsoids. Na1–Na5 were refined with anisotropic thermal parameters, whereas the disordered set was kept isotropic. Also, of the 26 waters of hydration in the asymmetric unit, only 16 at full occupancy and eight at half-occupancy were located. No hydrogen atoms were located or included in the structure factor calculation. The formula is reported below with the expected number of hydrogen and oxygen atoms. Crystal data: $H_{108}Co_4Na_{16}O_{166}P_4W_{30}$, $M_w = 9007.80$ amu, triclinic, $P\bar{1}$, $a = 13.6359(19)$, $b = 13.795(3)$, $c = 21.527(3)$ Å, $\alpha = 91.069(3)$, $\beta = 95.829(2)$, $\gamma = 118.226(2)°$, $V = 3539.2(10)$ Å^3, $T = 100(2)$ K, $Z = 1$, $\rho_{calcd} = 4.226$, R_1 $[I > 2\sigma(I)] = 0.0640$, wR_2 (all data) $= 0.1771$, GOF (on F^2) $= 1.023$.

EPR spectroscopy: Perpendicular polarization ($B_1 \perp B_0$) is a standard continuous-wave (CW) EPR technique can detect both Kramers (half-integer spin) and non-Kramers (integer spin) electronic-spin systems. For resonances originating from integer electronic-spin systems, there is increased transition probability when the oscillating magnetic field component (B_1) is oriented parallel to the primary Zeeman field (B_0).[23] One does not expect significant spectral intensity from half-integer-spin systems.[23,24]

Parallel (9.39 GHz) and perpendicular polarization (9.69 GHz) continuous-wave EPR data were collected on a Bruker ECS 106 X-band spectrometer equipped with an ER-4116DM dual mode cavity. Slow-passage conditions were met with scan rates between 9.6 and 16.7 mT s^{-1}. All spectra were recorded at 6 K under non-saturating power conditions.

All samples were run as frozen aqueous solutions and freezing was stepwise at ≈2 s per step or ≈30 s overall. Cryogenic temperatures were achieved using an Oxford Instruments ESR900 liquid-helium-flow cryostat and set using an Oxford Instruments ITC503 temperature and gas-flow controller. A modulation amplitude of 0.8 mT, modulation frequency of 100 kHz, conversion time of 40.96 ms and time constant of 40.96 ms were used for all data collection. Reported spectra are the average of ten scans.

X-ray absorption spectroscopy (XAS): Co K-edge XAS spectra were recorded on the multipole wiggler XAS beam-line 12 ID at the Australian Synchrotron, in operational mode 1.[25] The beam energy was 3.0 GeV and the maximum beam current was 200 mA. The energy scale was calibrated using a Co foil as an internal standard for which the calibration energy, 7709.0 eV, corresponds to the first inflection point of the foil. The "Average" program[26] was used to average raw data files, and exclude channels.

Fluorescent-mode XAS data were taken on both **1** and **2** in both solid and solution state at 10 K using a He closed-cycle cryostat. Solid-state samples were prepared by mixing with boron nitride and ground to a uniform fine powder, which was then loaded into 1 mm-thick Al spacers and sealed with 63.5 μm Kapton tape windows. Solution samples were prepared from 2 mM stock solutions of **1** and **2** to which 20% glycerol was added prior to pH adjustment. The pH of the solutions was adjusted with either a 0.05 M solution of NaOH or 0.05 M $HClO_4$, which were then frozen in liquid nitrogen prior to introduction to the cryostat. The program PySpline[27] was used to background subtract data, spline the data and calculate the Fourier transform of the EXAFS. An E_0 value of 7725.0 eV used when defining the k-range of the EXAFS. A four-segment spline of order 2 was fit to the EXAFS region, and all data normalized to the edge jump at 7770 eV.

Results and Discussion

Spectroscopy on the solutes: EPR spectroscopy indicates that the four Co^{II} centers (each high-spin, $S = 3/2$) in the complex are ferromagnetically coupled,[28,29] yielding an system with an integer net electronic spin, consistent with previous work. Figure 5 shows the $B_1 \perp B_0$ EPR spectra **1**

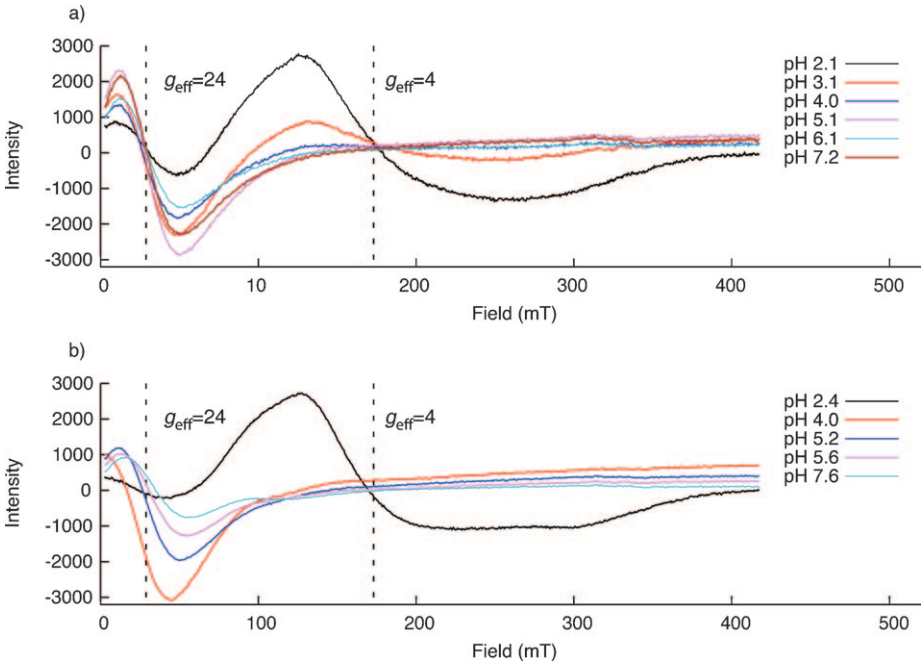

Figure 5. pH dependencies for perpendicular-mode EPR spectra of a) **1** and b) **2**. Total concentrations were ≈5 mM (**1**) and ≈2 mM (**2**). In both cases, the microwave frequency = 9.69 GHz, microwave power = 25.4 mW, and temperature = 6 K.

and **2** as a function of pH. At pH 7, a resonance is observed for **1** at $g_{eff} \approx 24$ and the line shape of this resonance is clearly stable to pH 5. The increase in intensity of the $g_{eff} \approx 24$ feature when polarization is changed from $B_1 \perp B_0$ to $B_1 || B_0$ (Figure 6) indicates that it is from an integer-spin system.

In strongly acidic solutions a second resonance becomes apparent at $g_{eff} \approx 4$ and the intensity increases as the pH decreases to pH 2. The change in these acidic solutions is highlighted in Figure 6a and b, in which the $B_1 \perp B_0$ and $B_1 || B_0$ spectra of complex **1** are presented for at pH 2.1 and 3.4. Two signals are present at $g_{eff} \approx 24$ and $g_{eff} \approx 4$ when the fields are perpendicular ($B_1 \perp B_0$). However, when spectra from the same samples are collected under $B_1 || B_0$ conditions, the resonance at $g_{eff} \approx 24$ increases in intensity, while the resonance at $g_{eff} \approx 4$ is no longer observed. Near disappearence of the signal at $g_{eff} \approx 4$ when $B_1 || B_0$ allows us to conclude that this signal arises from a Kramers electronic-spin system, in contrast to the signal at $g_{eff} \approx 24$.

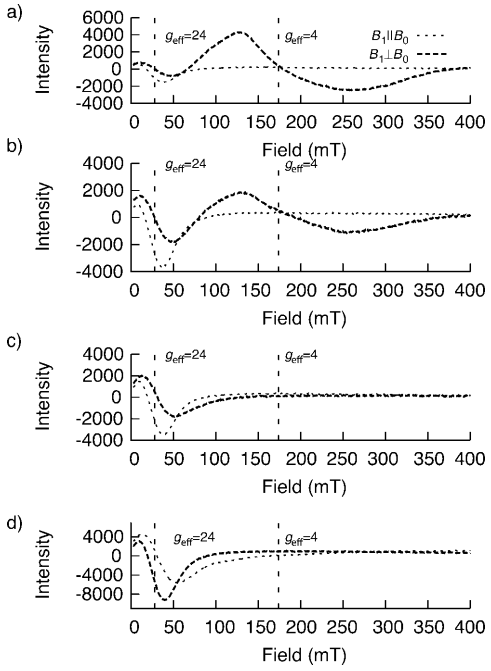

Figure 6. EPR spectra of compound **1** (≈5 mM concentration) acquired in parallel (dotted) and perpendicular (dashed) mode at: a) pH 2.1, b) pH 3.4 and c) pH 7. d) EPR spectra of compound **2** (≈2 mM at pH 5.6). The background electrolyte in all cases was 0.1 M $NaClO_4$. $B_1||B_0$ microwave frequency = 9.38 GHz, $B_1\perp B_0$ microwave frequency = 9.69 GHz, microwave power = 25.4 mW, and temperature = 6 K.

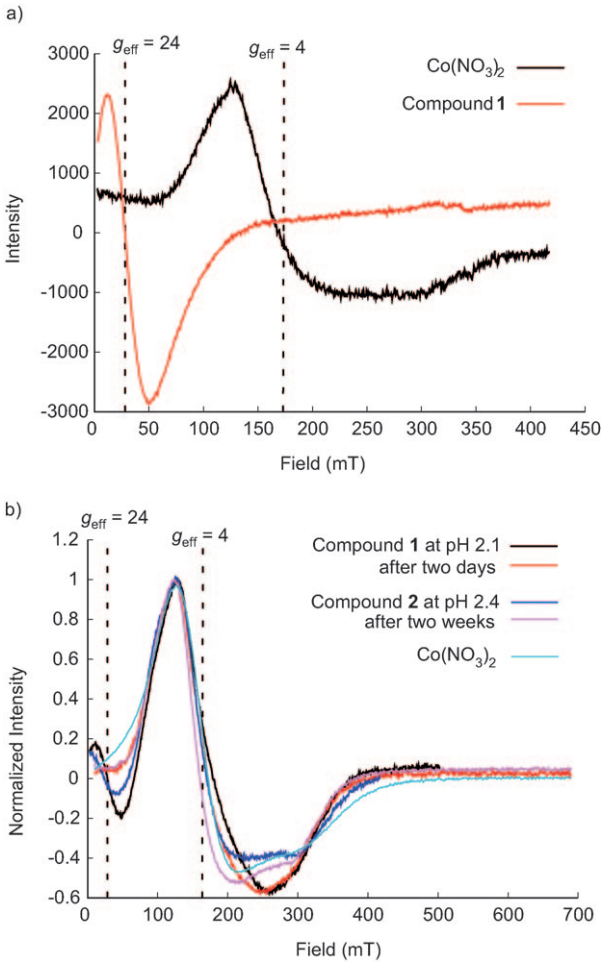

Figure 7. a) EPR signals for two solutions at pH 5. One was a solution of 2 mM of **1** (red) and the other (black) was a 1 mM $Co(NO_3)_2$ solution, both in 0.1 M $NaClO_4$. The EPR signals differ distinctly. These experimental conditions were chosen such that this concentration of $Co(NO_3)_2$ would give the same values of $\Delta\nu_{obs}$ as we observed in the ^{17}O-NMR spectra of **1** at pH 5. b) The EPR signals for **1** and **2** at low pH compare well to a $Co(NO_3)_2$ solution containing only $[Co(H_2O)_6]^{2+}$ (aq).

The EPR spectra of compound **2** are similar to **1**, but suggest slightly better pH stability. Figure 6c shows a comparison of the $B_1||B_0$ versus $B_1\perp B_0$ spectra obtained for **1** at pH 7, for which only the $g_{eff}\approx24$ signal is present, again indicating only a ferromagnetically coupled cobalt polyoxometalate species. However, at pH < 3 we observe the onset of a new signal corresponding to an uncoupled $S=3/2$ Co^{II} species, as was observed for **1**. Also at these low-pH conditions, the ^{31}P NMR spectra lack any of the signals associated with the αββα-**2** and αβββ-**2** complexes (see the Supporting Information).

The most reasonable interpretation is that both molecules are stable in slightly acidic solutions, but are dissociating in strongly acidic solutions to release $[Co(H_2O)_6]^{2+}$ ($S=3/2$). After two days at ambient-temperature conditions, the EPR spectra of **1** exhibit only the $g_{eff}\approx4$ signal, indicating the complete decomposition of the integer-spin complex, which reforms quickly upon pH reversal. Further experiments show that the $g_{eff}\approx4$ signal of complex **1** at pH 2.1 overlaps with the signal from a $Co^{II}(NO_3)_2$ solution (see Figure 7 and Supporting Information). The important point is that there is no evidence of the uncoupled $S=3/2$ system at slightly acidic conditions under which the kinetic measurements were made.

Of course, EPR spectroscopy alone cannot distinguish $[Co(H_2O)_6]^{2+}$ from some other cobalt complex with $S=3/2$, such as $[NaCo_3(H_2O)(P_2W_{15}O_{56})_2]^{17-}$. However, there is little evidence to support the idea that defect structures, such as $[NaCo_3(H_2O)(P_2W_{15}O_{56})_2]^{17-}$ or $[Na_2Co_2(P_2W_{15}O_{56})_2]^{18-}$,[15] are forming at low pH. These compounds have been reported to be dark violet and pink, respectively, and solutions of **2** are yellow-brown at pH 2.1 and the ^{31}P NMR spectra do not match those of the disodium dicobalt complex. Similarly, solutions of **1** at pH ≈ 2 are pink, which resembles more closely the color of $[Co(H_2O)_6]^{2+}$ than $[Na_2Co_2(PW_9O_{34})_2]^{12-}$, which is purple.[30] (The compound $[NaCo_3(H_2O)(PW_9O_{34})_2]^{11-}$ has not yet been isolated, but see reference [31] for a Ni^{II} version.)

The EPR results are supported by X-ray absorption spectra measured on aqueous solutions of **1** and **2**. XAS spectra were collected on both solids and solutions (Figure 8). In all cases, the XAS structural information are consistent with the crystallography and the XANES showing an energy shift and shape typical of Co^{II}. The Fourier transformed spectra of both **1** and **2** indicate two major peaks (Figure 8). The first peak is associated with the Co–O bonds and the second

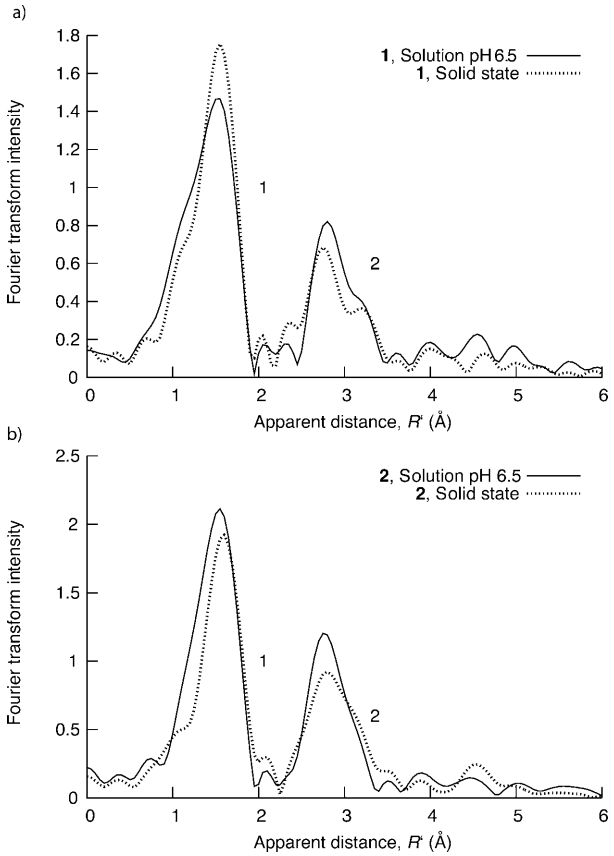

Figure 8. Fourier transform of the EXAFS data for a) **1** and **2** b) in solid state and as a frozen solution. Peaks 1 and 2 are referred to in the text.

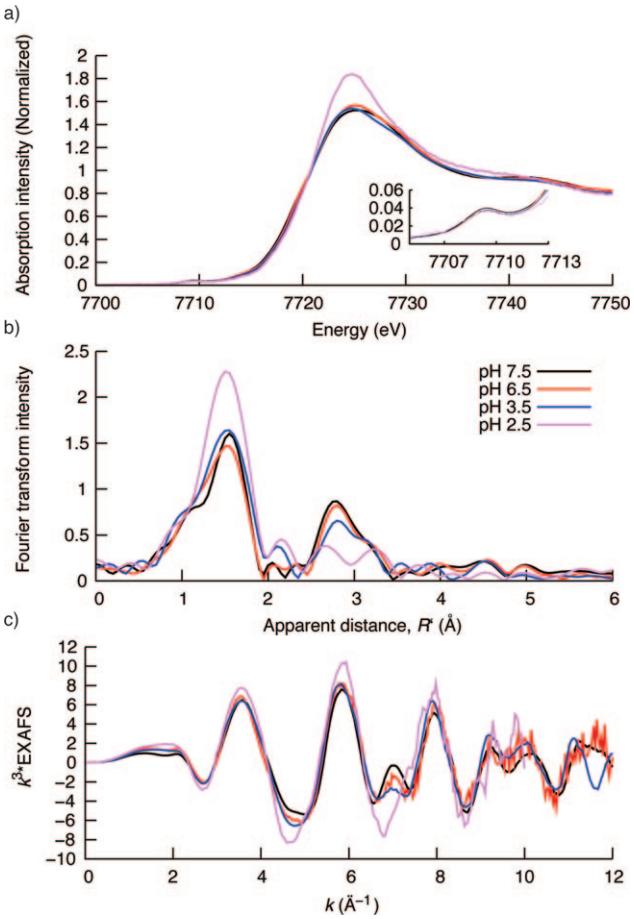

Figure 9. The pH dependence of the Co K-edge XAS spectra of **1**: a) XANES and pre-edge (inset); b) Fourier transform of the EXAFS; c) Fourier transform of the EXAFS. All data are shown for four pH conditions taken at liquid helium temperatures and frozen with glycerol.

associated with a disordered group of mainly single-scattering vectors assigned to Co–Co and Co–W. These are thought to become slightly less disordered on dissolution, as evident in the slight increase in the second peak of the Fourier transform. Otherwise the solution- and solid-state EXAFS are consistent with each other, and with other data. XANES energy shift and shape are consistent with Co^{II} and do not change as a function of pH.

Most importantly, the EXAFS spectra for **1** are similar to one another at near-neutral pH conditions, indicating that this anionic cluster does not undergo any major geometric change, such as dissociation. Figure 9 shows the XANES, EXAFS, and Fourier transform of the EXAFS of **1** at pH 7.5, 6.5, 3.5, and 2.5. As the pH is reduced to 2.5, a reduction in the 2nd peak of the Fourier transform is accompanied by an increase in the first peak of the Fourier transform. Some intensity is still evident in the Fourier transform around $R' = 3$. This change is consistent with the cluster dissociating to free cobalt(II) in solution, as was also indicated in the EPR spectra discussed above, and inferred from the potentiometry (see also Figures S15–S18 in the Supporting Information.)

The data consistently indicate that the polyoxometalate clusters are stable in near-neutral and slightly acidic solutions, but dissociate in strong acidic solutions. The potentiometry and UV/Vis results indicate reversible titrations in the region $4 < pH < 7$, but exhibits hysteresis due to irreversible changes and the uptake of multiple protons at low pH, consistent with proton-enhanced dissociation of the Co^{II} sandwich at these conditions. In the case of **1**, the high proton uptake is accompanied by visible changes in solution color from dark purple to a light pink, which is reversible.

We also find evidence, albeit subtle, in the titration curves for two protonation events occurring on **1** and **2** when lowering the pH from 7 to 3, in agreement with published titrations on **2**.[32] We interpret this evidence to indicate acid–base reactions affecting the tungstate ligands and not the Co^{II}-bound water molecules. These should not dissociate until $pH > 8$, consistent with all other Co^{II} complexes (Table 1) and the NMR data (below). The UV/Vis spectra contained several isosbestic points in this pH range, but deconvolution of the pH-dependent UV/Vis titration curve using factor analysis showed that >99% of the variance was accounted by a single factor, consistent with the idea that only a single chromophore is present over most of the pH range. A second component was identified at the most

Table 1. pK_a values for some Co^{II} aquo ligands.[a]

	Ionic strength [M]	pK_a	Reference
$[Co(H_2O)_6]^{2+}$(aq)	varying	9.8–10.2	[37,38]
$[Co(H_2O)(Me_6tren)]^{2+}$	1.0	8.6	[39]
$[Co(H_2O)(Me_6tren)]^{2+}$	varying	8.8±0.04	[37]
$[Co(H_2O)(tren)]^{2+}$	1.0	9.75	[39]
$[Co(H_2O)(tren)]^{2+}$	varying	10.22±0.01	[37]
$[Co(H_2O)(tpa)]^{2+}$	0.1	8.54±0.03	[40]
$Co(H_2O)(tla)]^{2+}$	0.1	9.66±0.08	[40]
$[Co(H_2O)(papd)]^{2+}$	0.5	12.45	[41]
$[Co(H_2O)(papd)]^{2+}$	0.5	8.4±0.15	[42]

[a] Me_6tren = tris(dimethylamino)ethylamine; tren = tris(2-aminoethyl)-amine; tpa = tris(pyridin-2-yl)methylamine; tla = tris(6-methylpyridin-2-yl); papd = 1,5,8,11,15-penta-azapentadecane.

acidic conditions where it accounted, at most, for ≈0.5% of the variance (see the Supporting Information).

Kinetics of isotope exchanges at Co^{II}-bound water molecules: At slightly acidic conditions, ^{17}O-NMR line widths and peak positions (Figure 4) indicate that the two waters bound to Co^{II} in the sandwich of both polyoxometalates exchange with bulk waters at rates that are broadly comparable to the $[Co(H_2O)_6]^{2+}$ ion (Table 2). For **1** at pH 5.4, we

Table 2. Rate parameters for compounds **1** and **2** derived from ^{17}O-NMR data and assuming that there are two exchangeable waters bound to each molecule. The least significant digit given within the parentheses.

pH	k^{298} [10^6 s^{-1}][a]	$\Delta H^{\neq}$ [kJ mol^{-1}][a]	$\Delta S^{\neq}$ [J mol^{-1} K^{-1}][a]
compound **1**			
4.6	1.7(5)±0.2	35.5±0.2	−6.4±0.6
5.4	1.5(5)±0.3	39.8±0.3(5)	+7.1±1.2
6.0	1.5±0.2	24.6±0.2	−44.3±0.6
	$\Delta V^{\neq}$ = 5.6±1.6 cm^3 mol^{-1} at pH 5.5		
compound **2**			
4.5	1.2±0.1	32.0±0.1	−21.7±0.4
5.4	1.6±0.3	27.6±0.4	−33.3±1.3
6.3	1.9±0.32	17.3±0.2(5)	−66.3±0.9
	$\Delta V^{\neq}$ = 2.2±1.4 cm^3 mol^{-1} at pH 5.2		
$[Co(H_2O)_6]^{2+}$ (aq)			
	3.2(±2.)	46.9±1.2	37.2±3.7[35]
		$\Delta V^{\neq}$ = 6.2 cm^3 mol^{-1}	

[a] Values of k^{298} and the associated uncertainties were estimated from a line width measurement at 298 K and not by back-calculation from the Arrhenius rate law. Thus the linear uncertainties in the values of $\Delta H^{\neq}$, $\Delta S^{\neq}$, and $\Delta V^{\neq}$ are not exponentiated and assigned to k^{298}. The uncertainties assigned to $\Delta H^{\neq}$, $\Delta S^{\neq}$, and $\Delta V^{\neq}$ correspond to the errors of regression at the 95% confidence level. Please see the Supporting Information for the equations.

estimate: $k^{298} = 1.6 \pm 0.3 \times 10^6$ s^{-1}, $\Delta H^{\neq} = 39.8 \pm 0.35$ kJ mol^{-1}, $\Delta S^{\neq} = +7.1 \pm 1.2$ J mol^{-1} K^{-1} and $\Delta V^{\neq} = 5.6 \pm 1.6$ cm^3 mol^{-1}. For the Wells–Dawson sandwich cluster **2** at pH 5.54, we find: $k^{298} = 1.6 \pm 0.3 \times 10^6$ s^{-1}, $\Delta H^{\neq} = 27.6 \pm 0.4$ kJ mol^{-1} $\Delta S^{\neq} = -33 \pm 1.3$ J mol^{-1} K^{-1} and $\Delta V^{\neq} = 2.2 \pm 1.4$ cm^3 mol^{-1} at pH 5.2. For comparison, the rate estimates for water exchange on $[Co(H_2O)_6]^{2+}$ range from 1–3.2 × 10^6 s^{-1}, $\Delta H^{\neq}$ = 47 kJ mol^{-1} and $\Delta S^{\neq} = 37$ J mol^{-1} K^{-1}. The data are highly reproducible, save for the highest temperatures examined (Figure 4), at which there is some hysteresis in the line widths; data from this temperature was not used to estimate rate coefficients. It is of interest to note that while the changes in activation enthalpies were consistent across pH and compound, the behavior of the activation entropy was much less so. While entropy is very sensitive to assumptions about concentrations and absolute rates, the data was found to be highly reproducible. The effects are thus reliable, but lack a trivial explanation, and would make a compelling future study.

The similarity in reactivity to the $[Co(H_2O)_6]^{2+}$ ion cannot be attributed to dissociation products of either **1** or **2**. Besides the spectroscopic evidence discussed above indicating that the solutions are stable and monospecific, the ^{17}O-NMR calculations are quite sensitive to the concentration of bound waters through the P_m factor. Consider the following example. We collected the following ^{17}O data for **1** at 298 K and pH 5: $\Delta\nu_1 = 93.1$ Hz; $\Delta\nu_{H_2O} = 45.5$ Hz. The molar concentration of **1** was 0.002 M and the corresponding concentration of bulk water was 55.56 M. At that temperature, the rate can be calculated from Equation (5).

$$\frac{\pi\left|\Delta\nu_{H_2O} - \Delta\nu_1\right|}{P_m} = k_{ex} \qquad (5)$$

Entering the known concentration of **1** and assuming a two-site exchange mechanism of Equation (2), we calculate a value of $k^{298} = 2.1 \times 10^6$ s^{-1}. At these conditions, we know from the EPR and XAS data that the dominant species in solution is **1** and that no signal at all is observed for $[Co(H_2O)_6]^{2+}$ ion.

However, if only five percent of **1** has dissociated to form $[Co(H_2O)_6]^{2+}$ with six bound waters to exchange, the P_m value would have been so altered that the line widths would have indicated $k^{298} = 1.4 \times 10^7$ s^{-1}. In other words, the effect of dissociation on the line broadening would have been easily discernable. The increased signal would have been well outside the experimental error and the value of k^{298} would have been unreasonably high (k^{298} for $[Co(H_2O)_6]^{2+}$ is a factor of ≈4 smaller).

These results also support our supposition that the Ruhlmann et al.[32] incorrectly assigned the pK_a values of the two waters bound to the Co^{II} site in **2** as being pK_{a1} = 3.5 and pK_{a2} = 5.3. Values of pK_a as low as pH 3.5 would be highly anomalous for Co^{II} complexes, or any divalent metal, and would have been more consistent with waters bound to trivalent metals.[33] There is no evidence that tungstate ligands are sufficiently electron-withdrawing to change the pK_a values by so much that pK_a < 4. Furthermore, the Co–O bond length to the unique Co^{II}-bound water, (O31), in **1** is 2.116(6) Å and in **2** the unique water is O57, with a Co–O bond length of 2.086(13) Å (Supporting Information). For comparison, the Co–O bond length is 2.08 Å in the $[Co(H_2O)_6]^{2+}$(aq) ion,[34] which has pK_a ≈ 10 (Table 2). The alternative, that the water molecules had converted to bound

hydroxyl groups, would have drastically suppressed the rates of exchange and introduced a conspicuous first-order pH dependence on rates in the near-neutral pH region, which was not observed (Table 2). Thus, the most reasonable interpretation is that the pK_a values for waters bound to Co^{II} in **1** and **2** are ≈ 8. It should be noted that Ruhlmann et al did not offer any supporting evidence for their assignment of pK_a.[32]

In Figure 7a, we show EPR data for two samples, one of which (red line) corresponds to a solution of **1** at pH 5, for which we derived k^{298} values and activation parameters. The second solution was prepared with $[Co(OH_2)_6](NO_3)_2$ added to broaden the ^{17}O-NMR line width until the values of $\Delta\nu_{obs}$ were equal to those in the ^{17}O-NMR experiment in the kinetic experiment. As can be gleaned from the figure, addition of this amount of $[Co(H_2O)_6]^{2+}(aq)$ ion would be impossible to miss in the EPR spectra because of the enormous growth of the $g_{eff} \approx 4$ signal (Figure 7). The EPR signals of the two samples are so distinctly different that the presence of a partly dissociated **1** would have been detected. Thus, we are confident that our rate data correspond to waters bound to the sandwich compound and not to the $[Co(H_2O)_6]^{2+}$ ion.

The $\Delta V^{\neq}$ values for **1** and **2** were determined at 293.3 K by measuring ^{17}O-NMR line widths at pressures from 5 to 250 MPa at two pH conditions (pH 3.15 and pH 5.5) (Figure 4). In the higher pH solution, there was no evidence of dissociation of the sandwich as measured by potentiometry, EPR spectroscopy, or by drift of the ^{17}O-NMR line width. For the pH 5.5 experiment with **1**, $\Delta V^{\neq} = 5.6 \pm 1.6\ cm^3\,mol^{-1}$. For **2**, the activation volume was much less certain than for **1**, with an activation volume of $2.2 \pm 1.4\ cm^3\,mol^{-1}$. The large relative uncertainty originates from the small changes in line width with pressure (Figure 4) relative to the diamagnetic standard. Even with the uncertainties, these data are broadly similar to that of $[Co(H_2O)_6]^{2+}$: $6.1 \pm 0.2\ cm^3\,mol^{-1}$.[35] To test whether pressure causes decomposition of **1**, a 5 mM sample was kept at a pressure of 250 MPa overnight and no line broadening was observed. In similar high-pressure experiments for **2**, we could also demonstrate that the molecule was stable by ^{31}P NMR measurements (Figure 4). There was no evidence of decomposition at pH 5.25.

Positive activation volumes are traditionally interpreted to suggest pathways with a interchange or mildly dissociative character using the formalism of Langford and Gray.[36] We are aware, and concerned, that this formalism was largely derived for monomeric metal ions in octahedral coordination[18] and may not be appropriate for polyoxometalate geometries. However, these are the first such measurements on a polyoxometalate structure and need comparison to an existing framework. With these caveats, the values are well away from the limiting volume assignable to a purely dissociative pathway of $\approx 13\ cm^3\,mol^{-1}$[18] for octahedral metal aqua ions.

Conclusion

A wide range of spectroscopic and potentiometric data indicate the sandwich molecules are stable at slightly acidic or near-neutral pH and that the solutions are monospecific–Co^{II} is present only in the sandwiches and does not exist with large amounts of defective sandwich structures or monomeric species. The ^{17}O-NMR data are consistent with two bound water molecules that exchange with bulk waters at similar rates to the $[Co(H_2O)_6]^{2+}$ ion. Such a result is consistent with the similar $\langle Co{-}OH_2 \rangle$ bond lengths for the sandwich structures and the monomeric aqua ion.

These are the first such data on polyoxometalate ions and so we can speculate about the broader trends in reactivity that might be observed for other, similar structures. First, coordination of the sandwich to the tungstate ligands apparently has little effect on the kinetics of reaction at the bound water molecules, which suggests that water molecules bound in similar planar brucite-like structures might also exhibit a similar result. Secondly, the small but reproducible and systematic variations in rates as pH rises probably reflect real changes in the sandwich structure, or its solvation, with solution composition. Such variations are also implied by the XAS and EPR spectra and will be worthy of future investigation.

Finally, the work is also significant because **1** catalyzes the oxidation of water in the presence of an electron acceptor, while **2** does not.[8] The reason for this difference does not seem to be attributable to any ligand effects on the terminal cobalt atoms, as $\langle Co{-}OH_2 \rangle$ bond lengths and exchange rates are very similar between the two compounds **1** and **2**. It is, however, interesting to note that the compound with less acid tolerance, **1**, is the one which catalytic activity has been observed. We can only speculate about the cause of this enhanced catalytic activity, but the ease of transformation of **1** into another species may play a key role.

Acknowledgements

The authors thank three perceptive referees, as well as Dr. Travis Anderson for guidance through the complexities of the Wells–Dawson literature, Prof. Craig Hill and his research group for advice, Dr. Simon J. Teat and Dr. Christine M. Beavers for assistance with the synchrotron work for the crystal structures, and Dr. Chris Glover, Dr. Bernt Johannessen and Dr. Glyn Devlin for their help setting up the beamline for the XAS experiments. XAS data described herein were collected by using the Australian synchrotron and we acknowledge facility support for the experiments through proposal P2980. Support for this research came from the National Science Foundation through grant EAR 0814242, from the US Department of Energy Office of Basic Energy Science through grant numbers DE-FG03-96ER 14629 and DE-FG03-02ER15693, a DOE GAANN Fellowship (BQM), the Australian Research Council through the Australian Centre of Excellence for Electromaterials Science, and the Advanced Light Source, supported by the Director, Office of Science, Office of Basic Energy Sciences, of the U.S. Department of Energy under Contract No. DE-AC02-05CH11231, for beamtime. Support for M.K.F., as a student visiting UCD, was from the Materials Science of Actinides, an Energy Frontier Research Center funded by the U.S. Department of

Energy, Office of Science, Office of Basic Energy Sciences under Award Number DE-SC0001089.

[1] C. L. Hill, *J. Mol. Catal. A* **2007**, *262*, 2–6.
[2] R. Neumann, M. Dahan, *J. Am. Chem. Soc.* **1998**, *120*, 11969–11976.
[3] R. Neumann, M. Dahan, *Nature* **1997**, *388*, 353–355.
[4] C. L. Hill, T. M. Anderson, J. W. Han, D. A. Hillesheim, Y. V. Geletii, N. M. Okun, R. Cao, B. Botar, D. G. Musaev, K. Morokuma, *J. Mol. Catal. A* **2006**, *251*, 234–238.
[5] I. S. Lee, L. J. R. , S. B. Prusiner, J. G. Safar, *J. Am. Chem. Soc.* **2005**, *127*, 13802–13803.
[6] J. T. Rhule, C. L. Hill, D. A. Judd, R. F. Schinazi, *Chem. Rev.* **1998**, *98*, 327–357.
[7] C. L. Hill, *Compr. Coord. Chem. II* **2004**, *4*, 679–759.
[8] Q. Yin, J. M. Tan, C. Besson, Y. V. Geletii, D. G. Musaev, A. E. Kuznetsov, Z. Luo, K. I. Hardcastle, C. L. Hill, *Science* **2010**, *328*, 342–345.
[9] A. Sartorel, M. Carraro, G. Scorrano, R. De Zorzi, S. Geremia, N. D. McDaniel, S. Bernhard, M. Bonchio, *J. Am. Chem. Soc.* **2008**, *130*, 5006–5007.
[10] C. G. Silva, Y. Bouiza, V. Formes, H. Garcia, *J. Am. Chem. Soc.* **2009**, *131*, 13833–13939.
[11] M. W. Kanan, D. G. Nocera, *Science* **2008**, *321*, 1072–1075.
[12] T. J. R. Weakley, H. T. Evans, Jr., J. S. Showell, G. F. Tourne, M. C. M. Tourne, *J. Chem. Soc. Chem. Commun.* **1973**, 139–140.
[13] R. G. Finke, M. W. Droege, P. J. Domaille, *Inorg. Chem.* **1987**, *26*, 3886–3896.
[14] R. Contant, *Inorg. Synth.* **1990**, *27*, 104–108.
[15] L. Ruhlmann, J. Canny, R. Contant, R. Thouvenot, *Inorg. Chem.* **2002**, *41*, 3811–3819.
[16] T. J. Swift, R. E. Connick, *J. Chem. Phys.* **1962**, *37*, 307–320.
[17] C. A. Eckert, *Annu. Rev. Phys. Chem.* **1972**, *23*, 239–264.
[18] T. W. Swaddle, *Inorg. Chem.* **1980**, *19*, 3203–3205.
[19] L. Helm, A. E. Merbach, *Chem. Rev.* **2005**, *105*, 1923–1959.
[20] A. Drljaca, C. D. Hubbard, R. Van Eldik, T. Asano, M. V. Basilevsky, W. J. Le Noble, *Chem. Rev.* **1998**, *98*, 2167–2289.
[21] G. M. Sheldrick, *Acta Crystallogr. Sect. A* **2008**, *64*, 112–122.
[22] T. M. Anderson, X. Zhang, K. I. Hardcastle, C. L. Hill, *Inorg. Chem.* **2002**, *41*, 2477–2488.
[23] M. P. Hendrich, P. G. Debrunner, *Biophys. J.* **1989**, *56*, 489–506.
[24] A. B. Abragam, B. Bleaney, *Electron Paramagnetic Resonance of Transition Ions*, Oxford University Press, Oxford, **1970**, p. 700.
[25] C. Glover, J. McKinlay, M. Clift, B. Barg, J. Boldeman, M. Ridgway, G. Foran, R. Garrett, P. Lay, A. Broadbent, *AIP Conf. Proc.* **2007**, *882*, 884–886.
[26] Average in Average, http://www.synchrotron.org.au/index.php/aus-syncbeamlines/x-ray-absorption-spectroscopy/data–analysis, Australian National Beamline Facility and the Australian Synchrotron, **2008**.
[27] A. Tenderholt, B. Hedman, K. O. Hodgson, *AIP Conf. Proc.* **2007**, *882*, 105–107.
[28] J. M. Clemente-Juan, E. Coronado, *Coord. Chem. Rev.* **1999**, *193–195*, 361–394.
[29] J. M. Clemente-Juan, E. Coronado, A. Gaita-Ario, C. Gimnez-Saiz, H.-U. Gudel, A. Sieber, R. Bircher, H. Mutka, *Inorg. Chem.* **2005**, *44*, 3389–3395.
[30] Y. Hou, L. Xu, M. J. Cichon, S. Lense, K. I. Hardcastle, C. L. Hill, *Inorg Chem.* **2010**, *49*, 4125–4132.
[31] U. Kortz, I. M. Mbomekalle, B. Keita, L. Nadjo, P. Berthet, *Inorg. Chem.* **2002**, *41*, 6412–6416.
[32] L. Ruhlmann, L. Nadjo, J. Canny, R. Contant, R. Thouvenot, *Eur. J. Inorg. Chem.* **2002**, 975–986.
[33] D. T. Richens, *The Chemistry of Aqua Ions*, Wiley, New York, **1997**, p. 59.
[34] K. Ozutsumi, K. Tohji, Y. Udagawa, S. Ishiguro, *Bull. Chem. Soc. Jpn.* **1991**, *64*, 1528–1532.
[35] Y. Ducommun, K. E. Newman, A. E. Merbach, *Inorg. Chem.* **1980**, *19*, 3696–3703.
[36] C. H. Langford, H. B. Gray, *Ligand Substitution Processes*, 2nd ed, Benjamin, New York, **1974**, p. 120.
[37] J. H. Coates, G. J. Gentle, S. F. Lincoln, *Nature* **1974**, *249*, 773–775.
[38] C. F. Baes, R. E. Mesmer, *The Hydrolysis of Cations*, Wiley, New York, **1976**.
[39] G. Anderegg, V. Gramlich, *Helv. Chim. Acta* **1994**, *77*, 685–690.
[40] G. Anderegg, E. Hubmann, N. G. Podder, F. Wenk, *Helv. Chim. Acta* **1977**, *60*, 123–140.
[41] M. Maeder, H. Macke, *Inorg. Chem.* **1994**, *33*, 3135–3140.
[42] L. Dadci, H. Elias, U. Frey, A. Hoernig, U. Koelle, A. E. Merbach, H. Paulus, J. S. Schneider, *Inorg. Chem.* **1995**, *34*, 306–315.

Received: December 8, 2010
Published online: March 17, 2011

